1973-12

Evaluation of the fracture postulate for viscoelastic materials.

Kapernick, Robert Edwin

Monterey, California. Naval Postgraduate School

EVALUATION OF THE FRACTURE POSTULATE FOR VISCOELASTIC MATERIALS

Robert Edwin Kapernick

NAVAL POSTGRADUATE SCHOOL
Monterey, California

THESIS

EVALUATION OF THE FRACTURE POSTULATE
FOR VISCOELASTIC MATERIALS

by

Robert Edwin Kapernick

Thesis Advisor: G. H. Lindsey

December 1973

Approved for public release; distribution unlimited.

Evaluation of the Fracture Postulate for Viscoelastic Materials

by

Robert Edwin Kapernick
Lieutenant, United States Navy
B.S., Montana State University, 1965

Submitted in partial fulfillment of the
requirements for the degree of

MASTER OF SCIENCE IN AERONAUTICAL ENGINEERING

from the

NAVAL POSTGRADUATE SCHOOL
December 1973

ABSTRACT

Experimental studies were conducted on unfilled viscoelastic materials to evaluate the fracture postulate which states that crack velocity is a unique function of stress intensity factor. To do this, fracture characterization tests were conducted for constant load, constant displacement, and constant displacement rate histories. A cyclic study, a more sophisticated application of the constant displacement rate case, was also conducted as a further evaluation of the fracture postulate.

The analytical theory used in obtaining viscoelastic stress intensity factors was based upon linear theory and sharp crack geometries. Moderate correlation was obtained among all test cases, notwithstanding the presence of significant specimen strains and finite crack tip radii.

TABLE OF CONTENTS

LIST OF FIGURES

LIST OF SYMBOLS

b	Specimen Width, Centerline to Boundary
c	Crack Length
$\dot{c}$	Crack Velocity
K_1	Elastic Stress Intensity Factor, Opening Mode
K_1^v	Viscoelastic Stress Intensity Factor, Opening Mode
V_o	Boundary Displacement, Measured from Specimen Centerline
F	Applied Load
E_{REL}	Relaxation Modulus
$R=dV_o/dt$	Boundary Displacement Rate, Measured from Specimen Centerline
t	Time
E_i, α_i, E_R	Constants Used to Fit Relaxation Modulus Curve
T	Temperature
A	Specimen Cross-Sectional Area
K	Amplitude of Basic Cycle, Cyclic Case
L	Period of Basic Cycle, Cyclic Case
a_T	Experimental Time-Temperature Shift Factor
ρ	Crack Tip Radius

ACKNOWLEDGEMENTS

Professor Gerald H. Lindsey developed the theory and provided the direction throughout this work. Bob Moeller designed and built the temperature chamber. Their professional assistance was indispensable.

I. INTRODUCTION

Over the years, fracture studies have led to the development of relationships among geometry, loading and crack length that prevail at the incidence of rupture and the onset of crack propagation. It has been found useful to define a stress intensity factor, K_1, which increases as the load on the specimen increases until a critical value, K_{1C}, is reached. At this point the crack rapidly propagates, and it has been found that K_{1C} is a material property, such that in every structure when this condition is reached, the crack becomes unstable.

In viscoelastic materials, the crack is found to propagate for almost any load level. The velocities are infinitesimally small for low loads and increase with increasing load. The question then becomes: at what velocity does the crack propagate for any given load, not at what load level does rapid crack propagation occur. A stress intensity factor for the viscoelastic case, K_1^v, can be obtained by the correspondence principle, where the stress intensity factor, K_1, for the elastic case in the Laplace transform domain is inverted into the time domain to give the viscoelastic stress intensity factor, K_1^v contains information relative to the specimen geometry, material, and boundary conditions.

The fracture postulate for viscoelastic materials can be stated in the following way:

$$\text{If} \qquad [K_1^v(t)]_{\text{BODY 1}} = [K_1^v(t)]_{\text{BODY 2}}$$

$$\text{then} \qquad [\dot{c}\ (t)]_{\text{BODY 1}} = [\dot{c}\ (t)]_{\text{BODY 2}}$$

Hertzler [Ref. 2] conducted constant stress and constant displacement tests on filled viscoelastic materials in an attempt to substantiate this relation. He developed fracture characterizations by plotting stress intensity factors versus crack velocities for each test. His results showed the constant displacement and constant stress fracture characterizations diverging with increasing stress intensity factor. This disparity was attributed to the dewetting behavior of the material.

This study makes a further attempt to prove the fracture postulate using an unfilled viscoelastic material, since unfilled materials do not experience dewetting. Fracture characterizations were developed, using the same procedure as Hertzler's, from three experimental tests: the constant load case, the constant displacement case, and the constant displacement rate case. A cycling application of the constant displacement rate test was also performed as an added history common to viscoelastic analysis and as a further test of the fracture postulate. These test results were then compared, to evaluate the fracture postulate.

II. EXPERIMENTAL EQUIPMENT

A. TEST SPECIMENS

The unfilled viscoelastic material used in testing was a carboxy terminated, polybutadiene (CTPB) polymer composed of 94.97% Butarez and 5.03% Hx868. The samples were fabricated by the Naval Weapons Center, China Lake, California.

The specimens were prepared for testing by cutting a three-fourths inch horizontal crack in the sample as shown in Figure 1. Specimens could then be used for crack lengths up to three inches with less than 1% difference between the far-field stress in the undisturbed region and the average stress based on net cross section [Ref. 1].

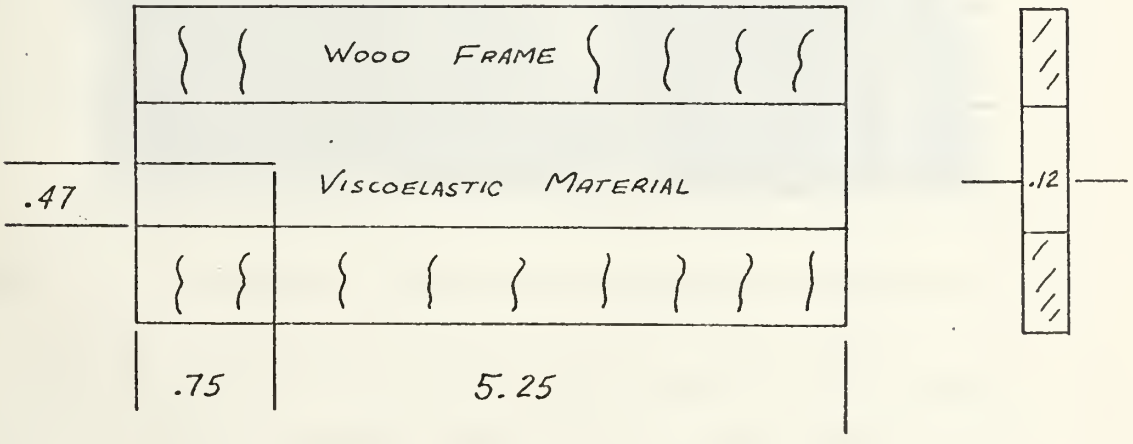

Figure 1. Geometry of Test Specimens

B. LABORATORY HARDWARE

Experimental testing was done with a table model Universal Instron. A temperature chamber was built to fit the Instron so that specimen temperature could be regulated during the test (see Figure 2). The Instron was equipped to directly conduct constant displacement, constant displacement rate, and cyclic tests.

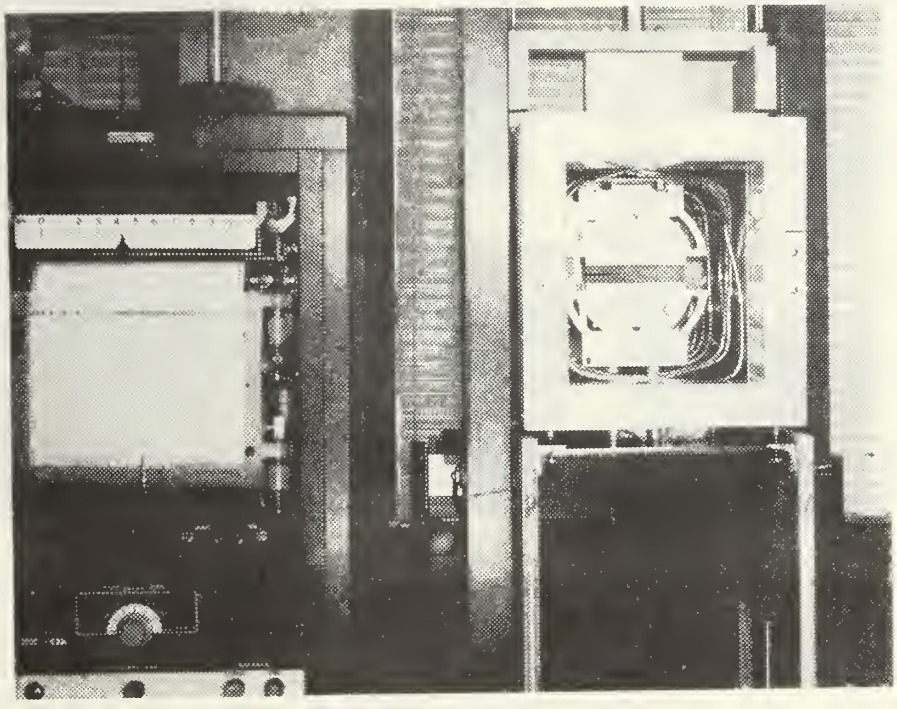

Figure 2. Universal Instron with Temperature Chamber.

For the constant load test, the apparatus was adapted (Figure 3) so a constant load could be suspended beneath the temperature chamber. Since this case required a uniform stress state on the loaded boundary, the apparatus was built so that the center of gravity of the applied

load could be maintained under the center of the uncracked length of the specimen. This provided a constant strain along the length of the specimen, insuring a uniform stress boundary condition.

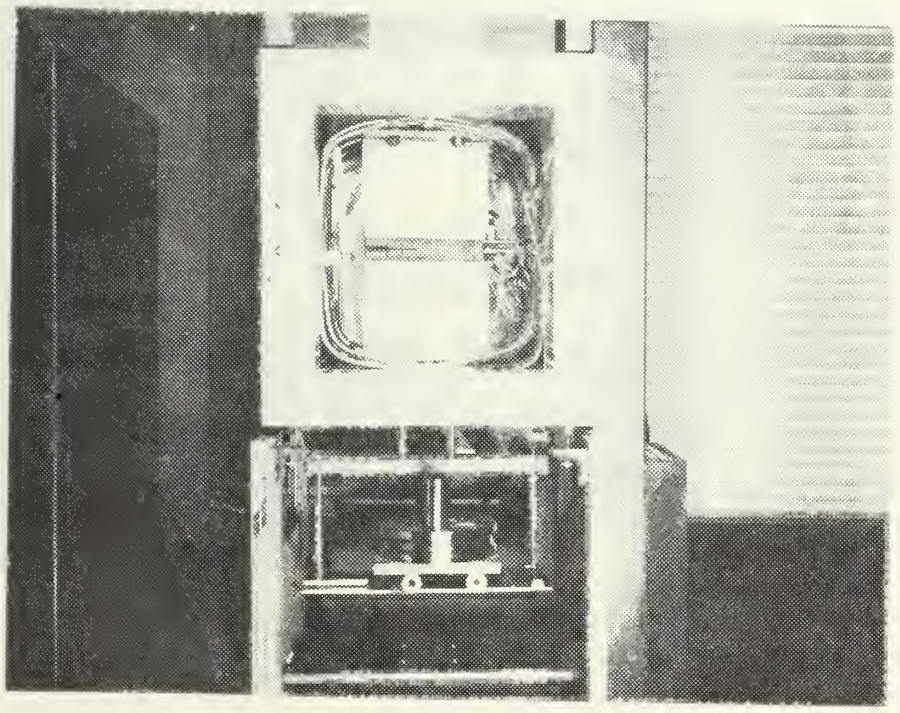

Figure 3. Universal Instron and Temperature Chamber Adapted for Constant Load Test

Specimen temperature was monitored with five thermistors each located one-eighth inch behind the sample and spaced so as to provide a thorough coverage of the material surface. Their locations are shown in the photograph of Figure 4.

Even though the temperature coils were exposed and located relatively close to the specimen ends, minimal temperature gradients occurred in the area of the test

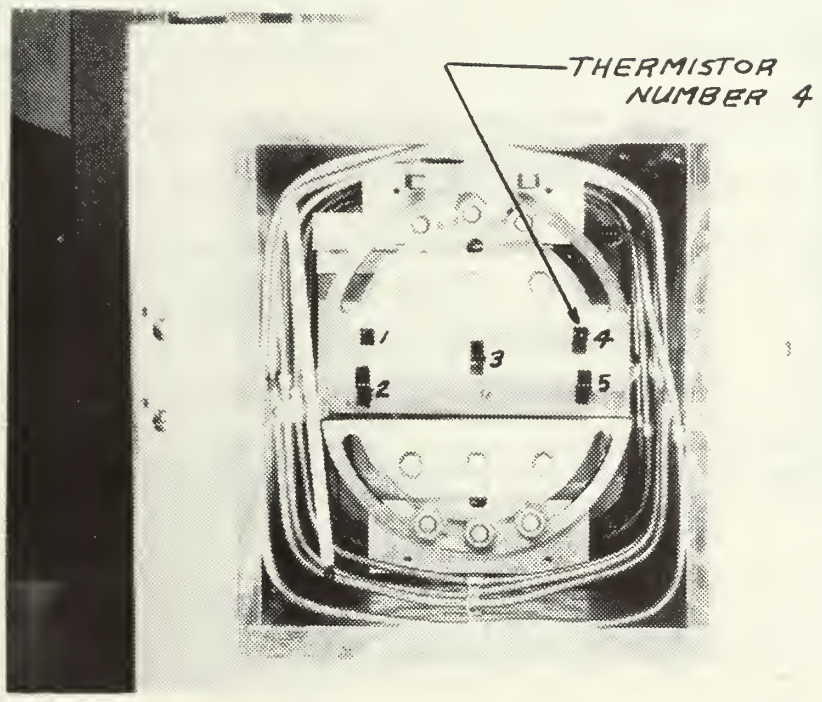

Figure 4. Temperature Chamber.

sample. The uniform temperature in the horizontal direction was attributed to the large metal fixture in the center of the chamber which acted as a heat sink, provided much thermal inertia, and tended to stabilize the temperature in its immediate vicinity. The temperature chamber had a substantial vertical temperature gradient, but this feature was not critical since the specimen dimension in this direction was small.

Temperature chamber statistics are given in Table 1. The "high" and "low" data represented the test specimen

environment at the maximum and minimum temperatures within the chamber during one cycle. This high-low-high chamber cycle took about five minutes for the 15, 30 and 50 degree temperatures, while the compressor ran for a longer portion of the cycle as the temperature decreased. At 70 degrees, the chamber was basically maintaining room temperature but providing a chamber environment. At zero degrees the compressor was continually running providing a relatively constant temperature.

TEST TEMPERATURE, °F	THERMISTOR NUMBER 1 LOW	1 HIGH	2 LOW	2 HIGH	3 LOW	3 HIGH	4 LOW	4 HIGH	5 LOW	5 HIGH
70	ROOM TEMPERATURE									
50	50.1	51.4	49.1	50.3	49.1	50.3	49.8	51.1	49.1	50.3
30	29.6	31.0	28.8	29.9	29.0	30.4	29.3	31.8	31.0	28.8
15	14.2	16.2	11.5	14.0	13.8	16.3	13.5	15.5	11.6	14.2
0	COMPRESSOR CONTINUALLY RUNNING									

TABLE I. Temperature Chamber Statistics

III. EXPERIMENTAL RESULTS

A. CONSTANT LOAD CASE

The viscoelastic stress intensity factor (opening mode) for the constant load case was found by Lindsey [Ref. 1] to be:

$$K_1^v(t) = \sqrt{\frac{3b(t)}{4\pi}} \quad \frac{F}{A(t)} \tag{1}$$

This test consisted of placing a step load on the sample, which was then maintained constant throughout the test. Load levels required to produce crack propagation created specimen strain levels from 20% to 40%. To provide a uniform stress on the loaded specimen boundary and to avoid introducing a moment at the crack tip as the crack propagated, the center of gravity of the applied load was continually moved so as always to be under the center of the uncracked length of the specimen. Slow crack velocities made this method tractable.

Since the specimen was finite in length, an increase in crack length resulted in a decrease in A(t) and an associated increase in material strain. This increased the sample width and, by Poisson's effect, reduced the sample thickness. With increasing crack length, then, the stress intensity factor increased, resulting in a history of stress intensity factors for one applied load.

For the constant load case, the increase in crack velocity with an increase in crack length was small. Therefore, the crack velocity was experimentally observed, and averaged about four times, during each test. The stress intensity factor was computed based on the average crack length for a particular crack velocity. Stress intensity factors versus crack velocities were then plotted for specific testing temperatures. Since the viscoelastic material was thermoreologically simple [Ref. 2], each temperature curve was ultimately shifted into a smooth master fracture characterization curve.

Individual temperature test results are given in Figure 5, and the master fracture characterization curve is given in Figure 6. Test data had relatively little scatter, and the experimental temperature shift factors had good correlation with relaxation modulus shift factors [see Figure 6].

B. CONSTANT DISPLACEMENT CASE

The viscoelastic stress intensity factor (opening mode) for a constant displacement case was found by Lindsey [Ref. 1] to be:

$$K_1^{V}(t) = \sqrt{\frac{4}{3b(t)\pi}}\ V_o\ E_{REL}(t) \qquad (2)$$

To obtain a constant displacement boundary condition, the specimen boundary was displaced at a rate of two inches per minute until reaching the desired displacement,

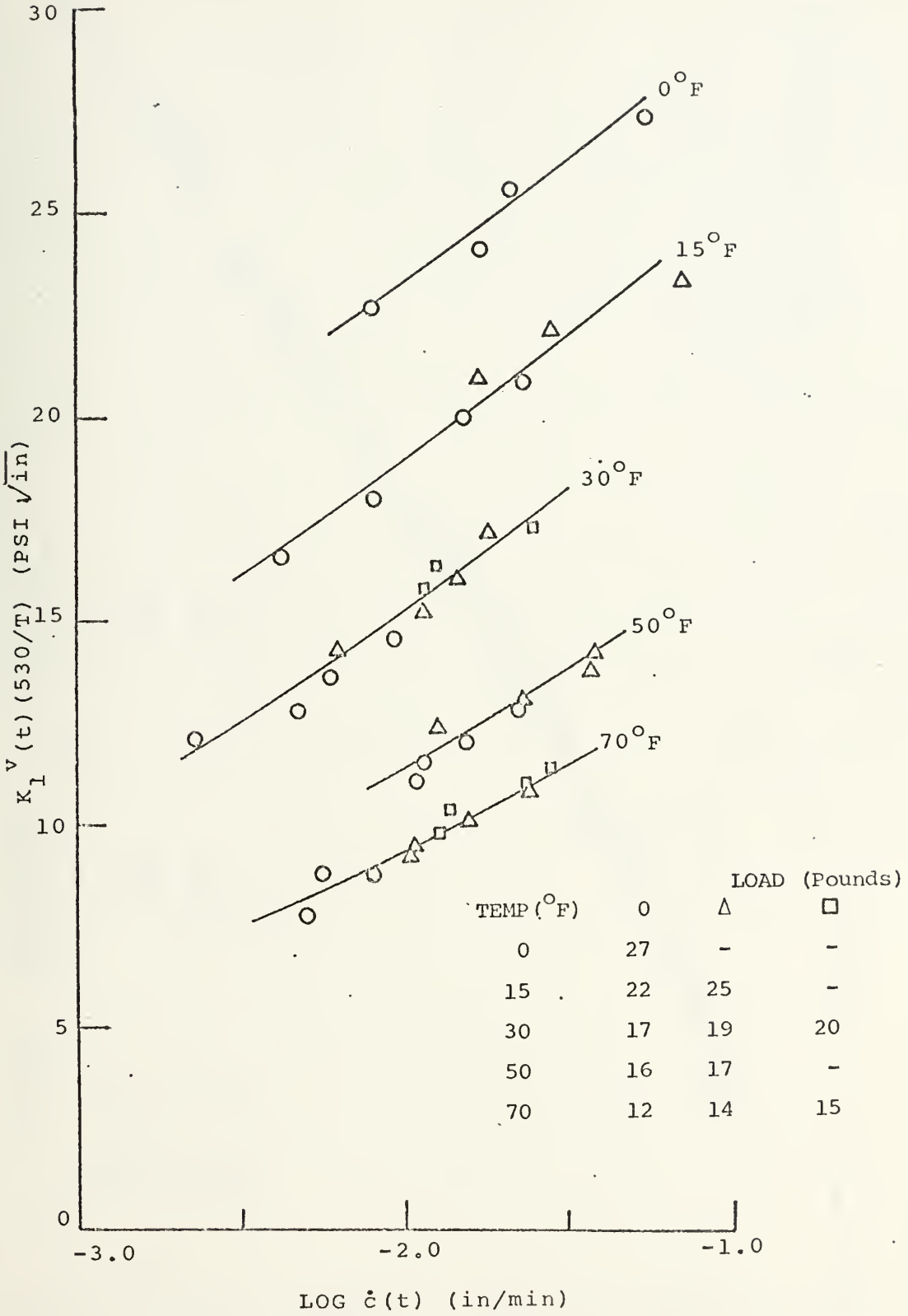

Figure 5. Fracture Characterization Curves for the Constant Load Case.

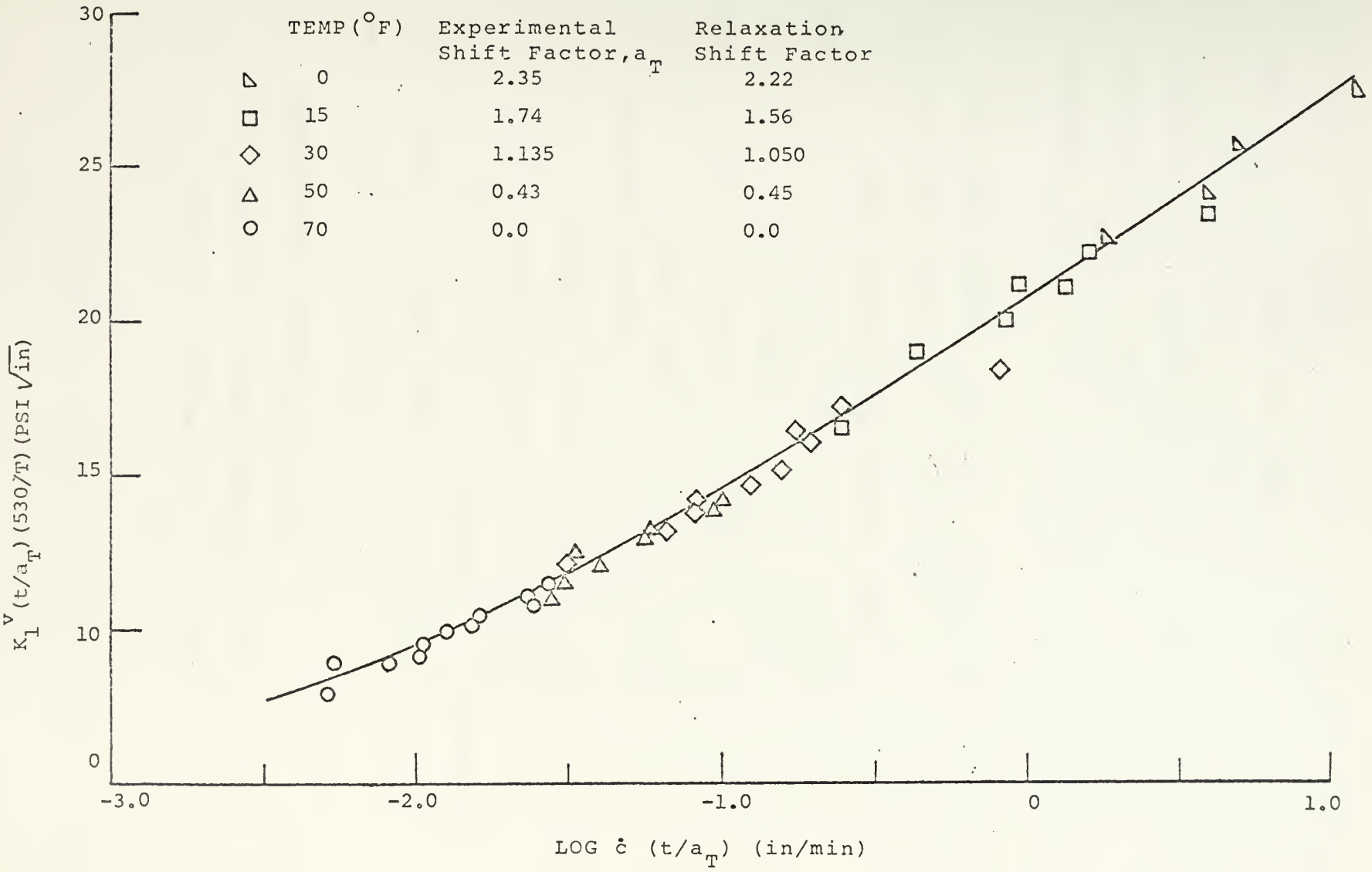

Figure 6. Fracture Characterization Master Curve for the Constant Load Case.

V_o. Then, by waiting ten times the loading time, the ramp tests simulated step displacement loading for which the stress intensity factor reduced to Equation (2). As time increased after loading, the stress intensity factor and corresponding crack velocity decreased as a result of relaxation. This yielded a history of fracture data from one test.

As in the constant load case, the crack velocity was experimentally observed and averaged over each time increment. Stress intensity factors were computed based on the average relaxation modulus for a particular crack velocity. Stress intensity factors versus crack velocities were plotted as a function of temperature, and finally shifted to a master fracture characterization curve.

Individual temperature test results are given in Figure 7 and Figure 8, and the master fracture characterization curve is given in Figure 9. Test data had a moderate degree of scatter, and experimental temperature shift factors had some disagreement with relaxation modulus shift factors [see Figure 9].

C. CONSTANT DISPLACEMENT RATE CASE

The viscoelastic stress intensity factor (opening mode) for a constant displacement rate case was found by Lindsey [Ref. 1] to be:

$$K_1^v(t) = \sqrt{\frac{4}{3b(t)\pi}}\ R\{\Sigma[\frac{E_i}{\alpha_i}(1- e^{-\alpha_i t})] + E_R t\} \qquad (3)$$

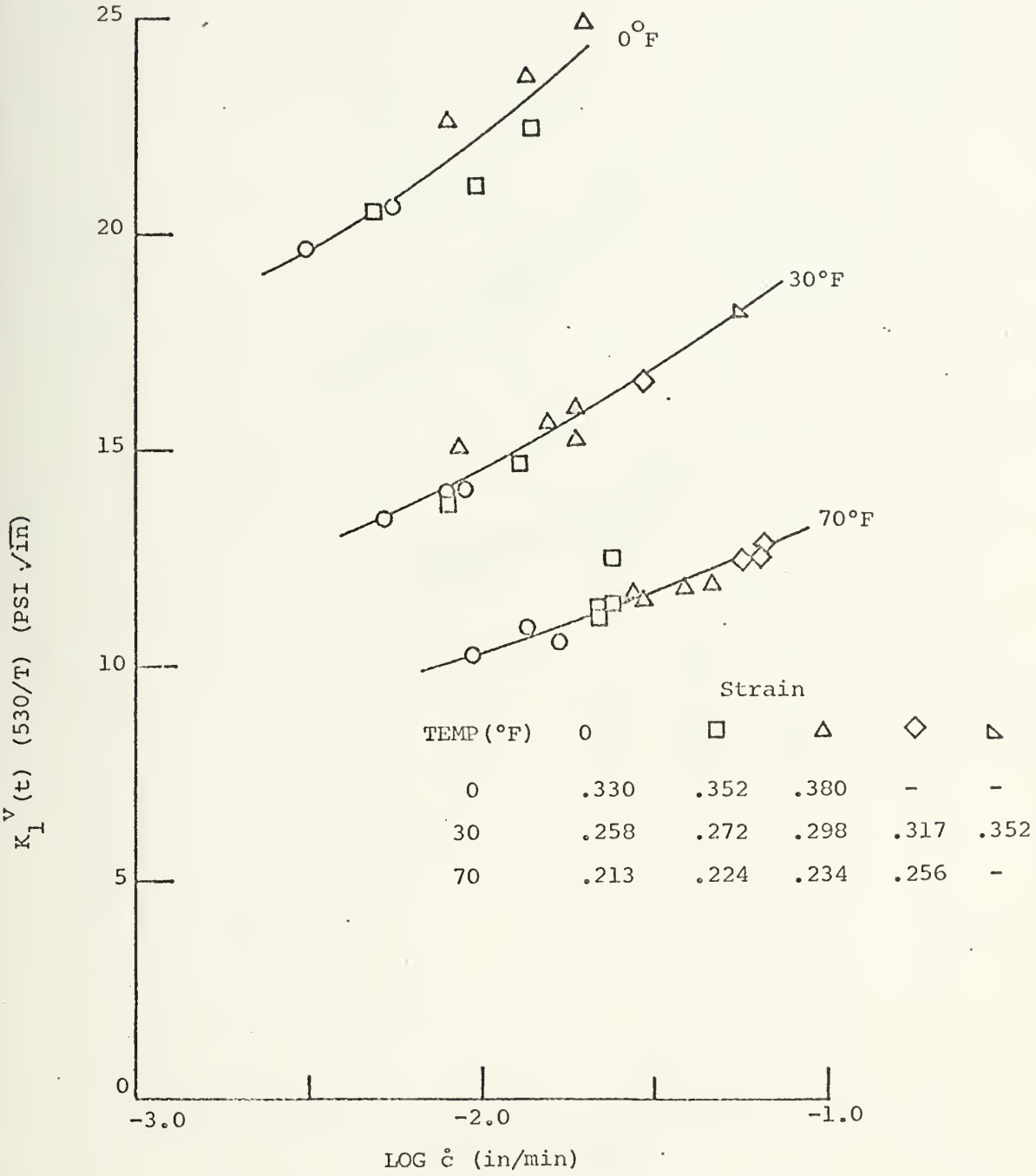

Figure 7. Fracture Characterization Curves for the Constant Displacement Case

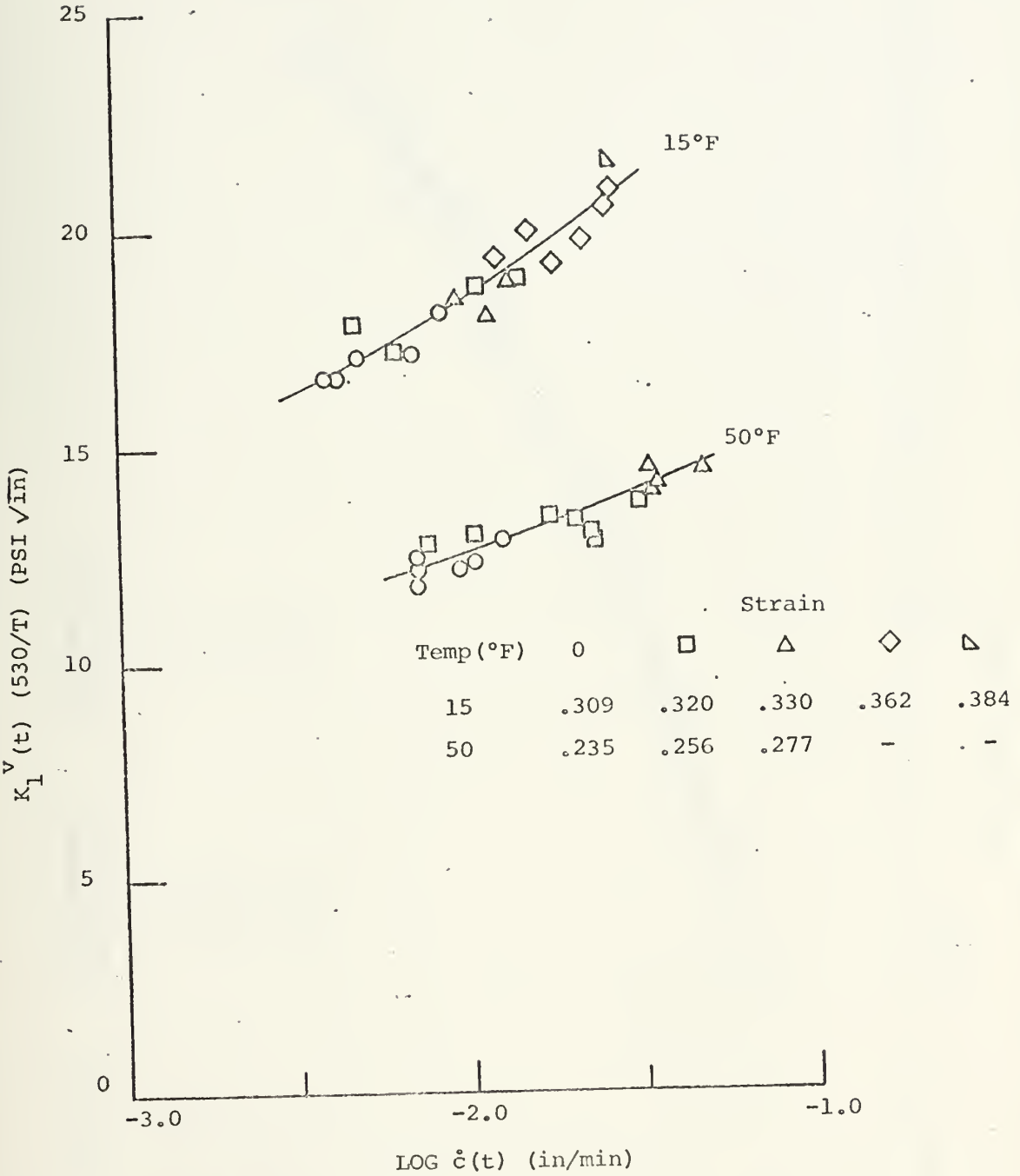

Figure 8. Fracture Characterization Curves for the Constant Displacement Case

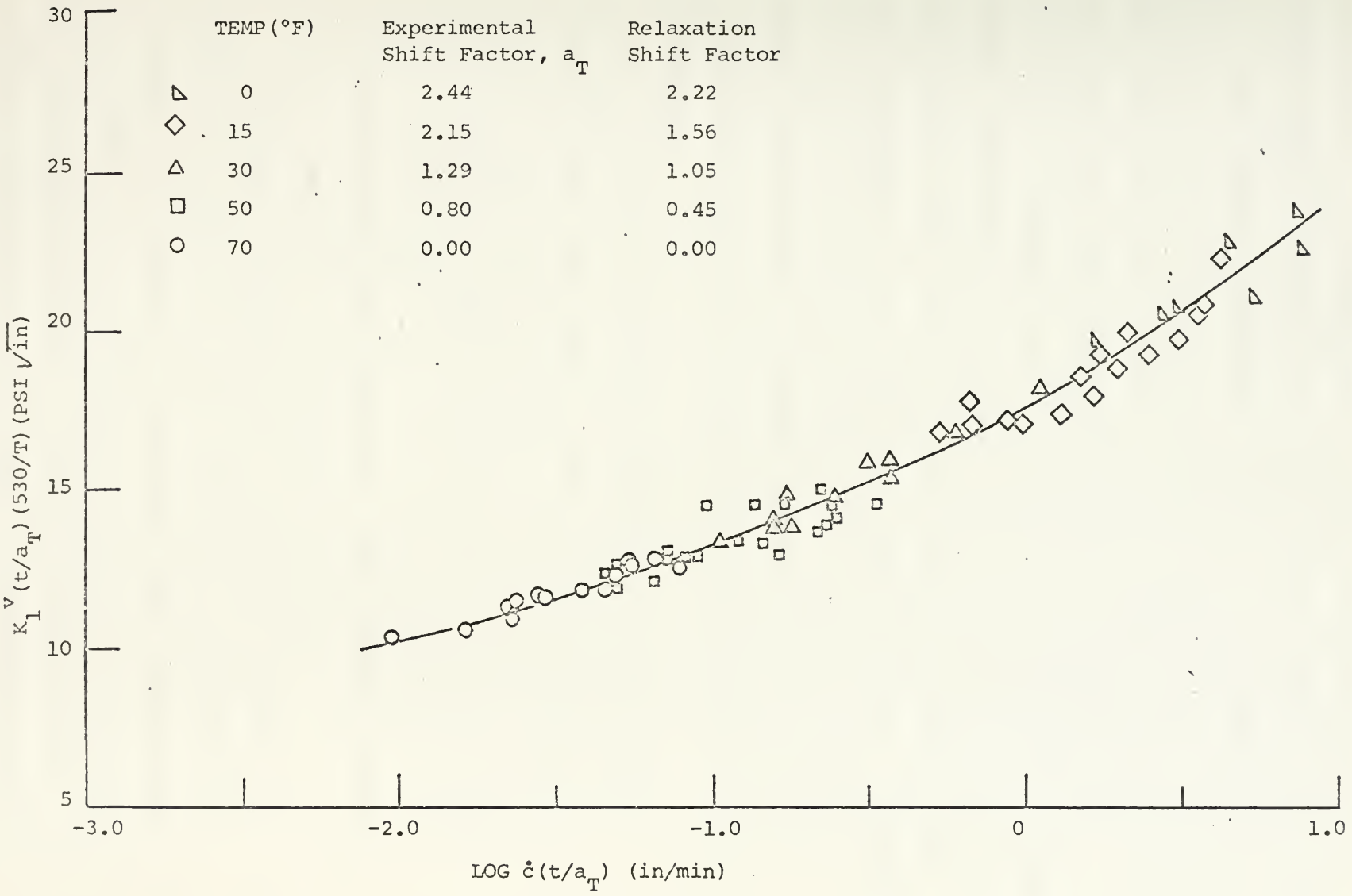

Figure 9. Fracture Characterization Master Curve for the Constant Displacement Case.

where E_i, α_i were determined by the procedure given in ICRPG Solid Propellant Mechanical Behavior Manual [Ref. 3].

The constant displacement rate test utilized the Instron in its most straight-forward application. One displacement rate was selected for the Instron crossarm, and this rate was maintained throughout the complete test. This test differed from the constant load test and the constant displacement test in two ways. First, one test generated a wide range of crack velocities, prohibiting the averaging of crack velocity during the test. Secondly, this extensive history of data from one test resulted in only three different constant displacement rates at one temperature being required for sufficient fracture characterization.

To accurately represent experimental data, crack lengths versus time were plotted. Fracture characterization was then done in two ways. First, crack velocities were graphically obtained by measuring the slope of the crack length versus time plots, and corresponding stress intensity factors were computed. This method permitted a direct comparison with previous results.

Secondly, recognizing the inaccuracy inherent in graphically obtaining crack velocities, an incremental technique was employed. The crack length-versus-time plot was divided into discrete time increments. Beginning at the first time increment, a stress intensity factor was computed from Equation (3), and a corresponding crack

velocity was obtained from the master fracture characterization curves. The current crack length was then obtained from the crack velocity by assuming it to be constant over the time increment. This process was continued and the resulting crack length-time history was compared with the experimental crack length-time history.

Experimental results based on graphically obtaining the crack velocity are given in Figure 10, labeled "Constant Displacement Rate." Crack length versus time plots are given for the three constant displacement rate tests in Figure 11, Figure 12, and Figure 13, and are labeled "Experimental, Constant Displacement Rate." A smooth, continuous crack length-versus-time curve resulted from the constant displacement rate test.

D. CYCLIC CASE

The basic equation for a viscoelastic stress intensity factor (opening mode) for the cyclic case was given by Lindsey [Ref. 1] as:

$$K_1^v(t) = \sqrt{\frac{4}{3b\pi}} \int_o^t E_{REL}(t - \tau) \frac{dV_o}{d\tau} d\tau \qquad (4a)$$

$$E_{REL}(t-\tau) = \sum E_i e^{-\alpha_i t-\tau)} + E_R \qquad (4b)$$

The cyclic case was an extension of the constant displacement rate case as one crossarm rate was maintained throughout the complete test. The direction of crossarm travel was reversed, however, when a selected displacement

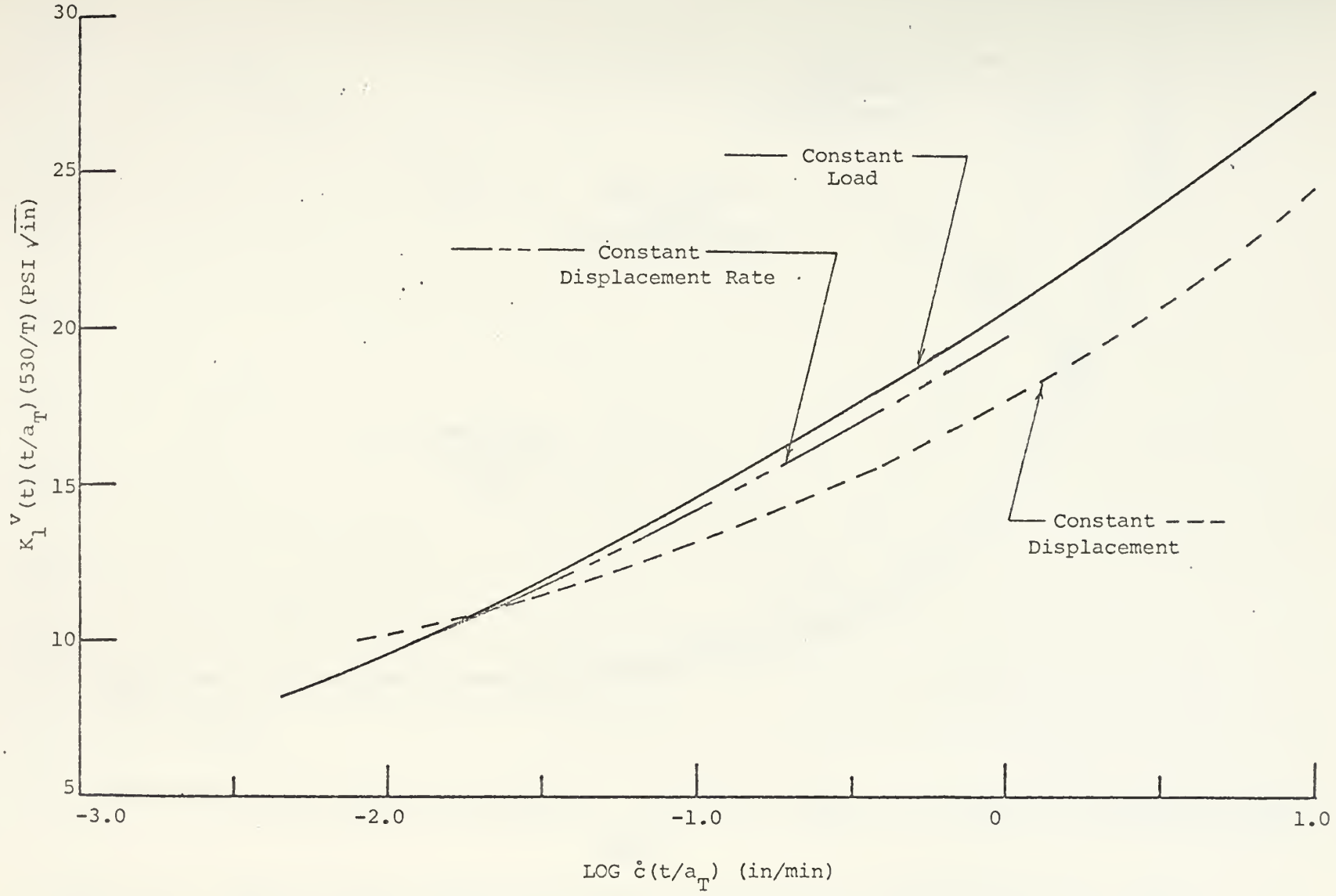

Figure 10. Summary of Fracture Characterization Master Curves.

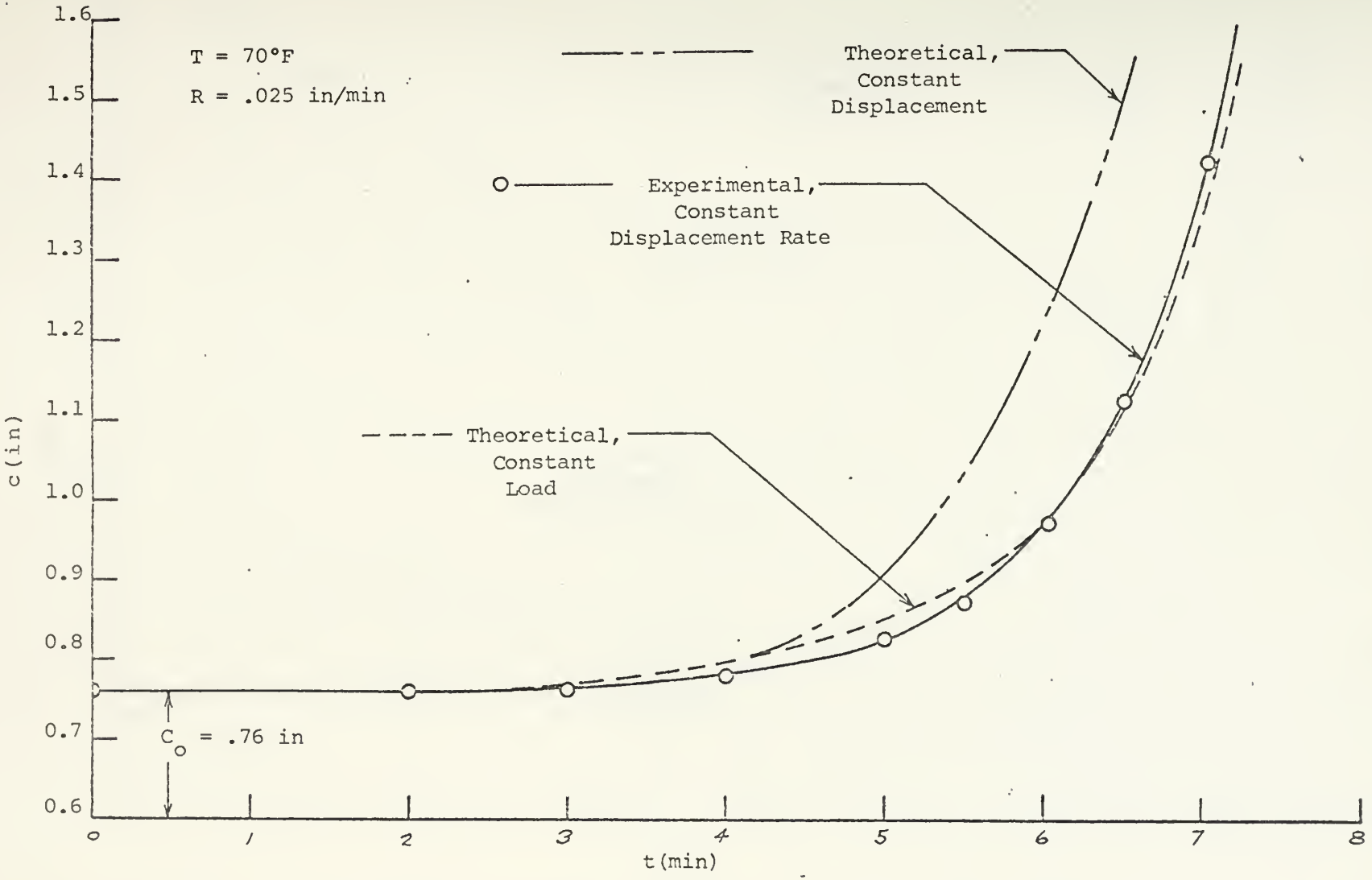

Figure 11. Crack Length versus Time for the Constant Displacement Rate Case

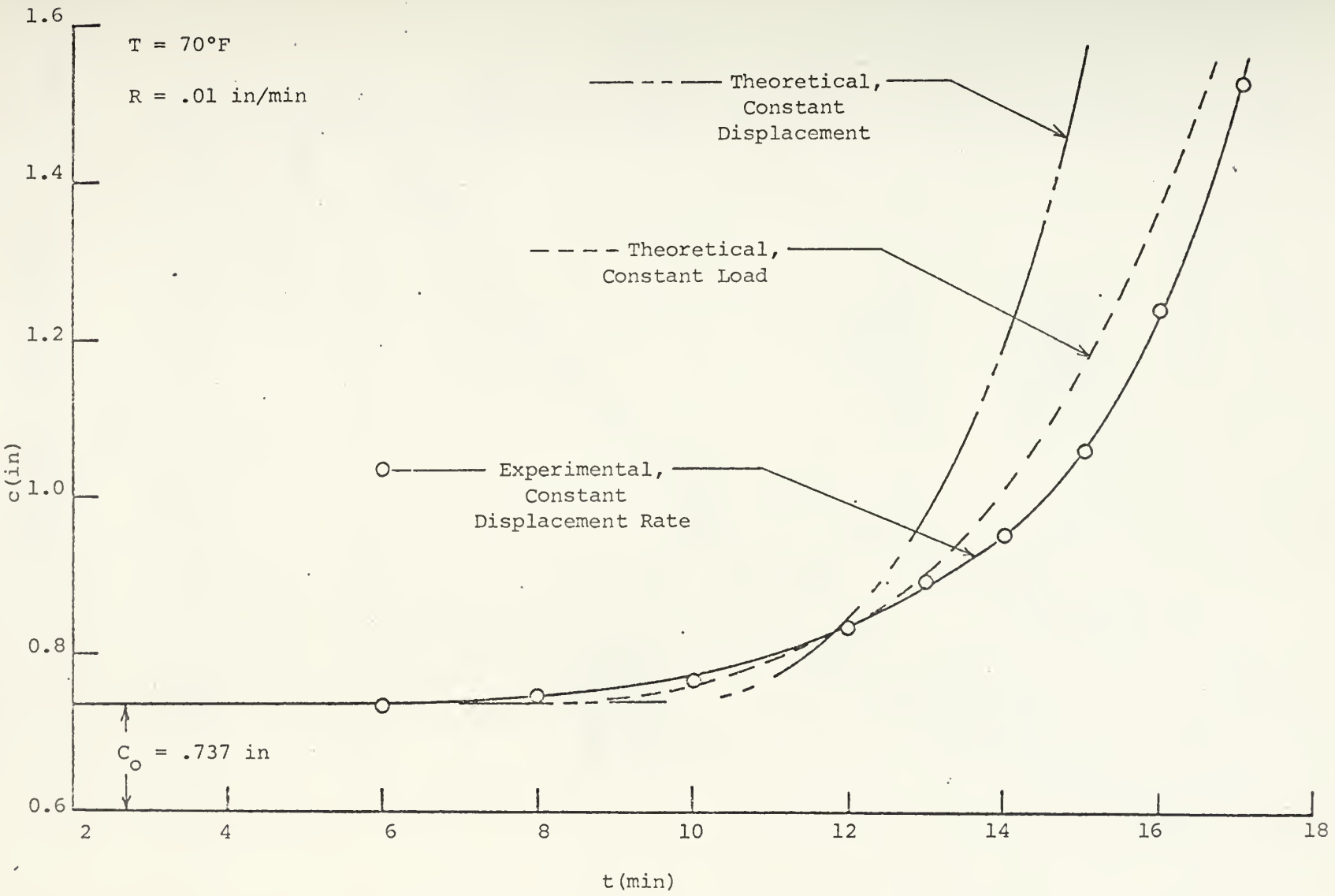

Figure 12. Crack Length versus Time for the Constant Displacement Rate Case

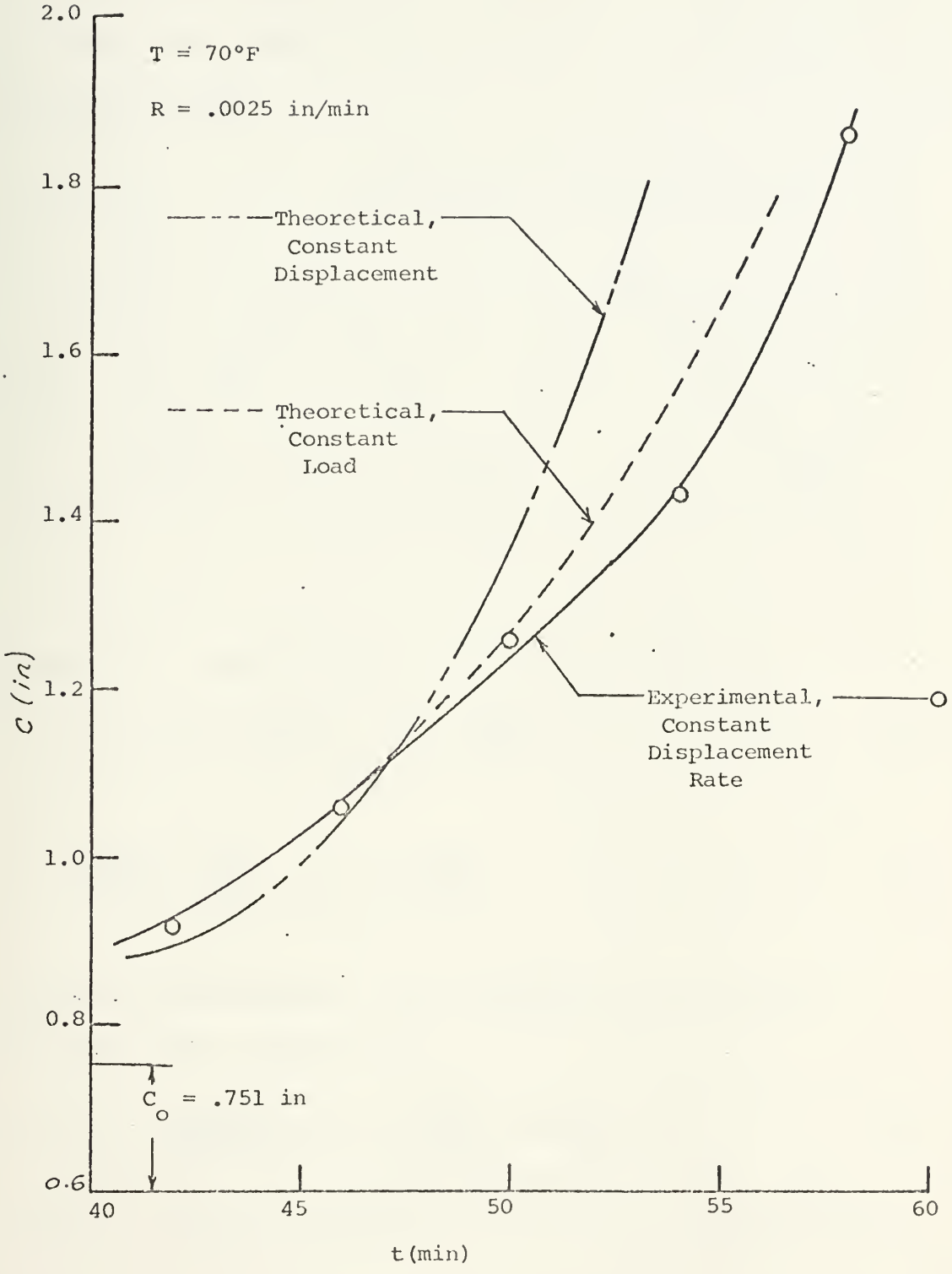

Figure 13. Crack Length versus Time for the Constant Displacement Rate Case

was reached. This resulted in a linear, piecewise continuous, even function which could be approximated by a Fourier series.

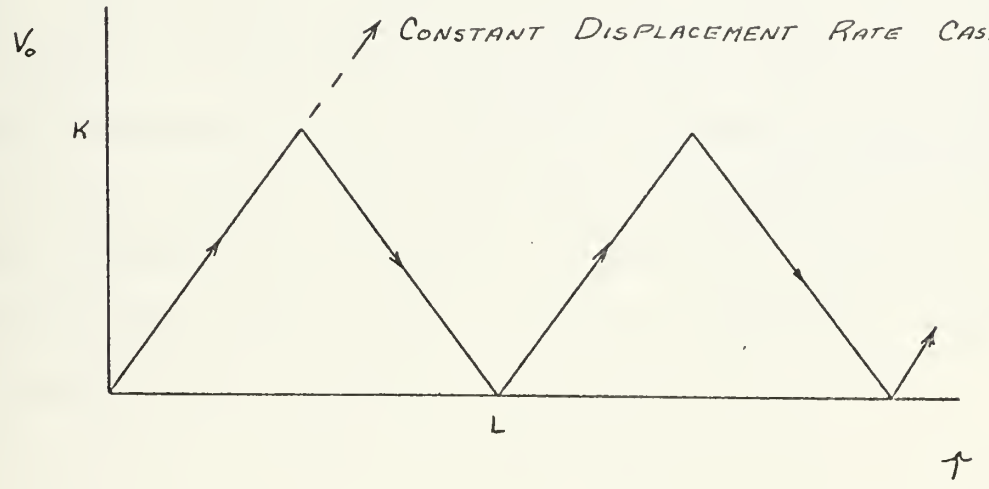

Figure 14. Basic Cycle for the Cyclic Test.

$$V_o(\tau) = \frac{K}{2} - \frac{16K}{\pi^2} \sum_n \frac{1}{n^2} \cos \frac{n\pi\tau}{L} \qquad n = 2, 6, 10 \qquad (5a)$$

$$\frac{dV_o(\tau)}{d\tau} = \frac{16K}{\pi L} \sum_n \frac{1}{n} \sin \frac{n\pi\tau}{L} \qquad n = 2, 6, 10 \qquad (5b)$$

Substituting Equation (5b) and Equation (4b) into Equation (4a) resulted in:

$$K_1 v(t) = \frac{16K}{\pi L} \sqrt{\frac{4}{3b(t)\pi}} \sum_n \left\{ \frac{-E_R L}{n^2 \pi} \left(\cos \frac{n\pi t}{L} - 1\right) + \right. \qquad (6)$$

$$\left. + \sum_i \left[\frac{E_i (\alpha_i \sin n\pi t/L - n\pi/L \cos n\pi t/L)}{n(\alpha_i^2 + n^2\pi^2/L^2)} + \frac{e^{-\alpha_i t} E_i \, n\pi/L}{n(\alpha_i^2 + n^2\pi^2/L^2)} \right] \right\}$$

$$n = 2, 6, 10$$

$$i = 1, 2, 3, \cdots, 9$$

Equation (6) was solved on the computer using 14 terms in the Fourier series.

Experimental data were plotted as crack length versus time. This was then compared with the constant load case and constant displacement case using the incremental procedure described in the constant displacement rate case.

A crack length-versus-time plot is given for a cycling test in Figure 15 (also shown in Figure 16), labeled, "Experimental, Cyclic Case." This test produced a stair-step crack length history.

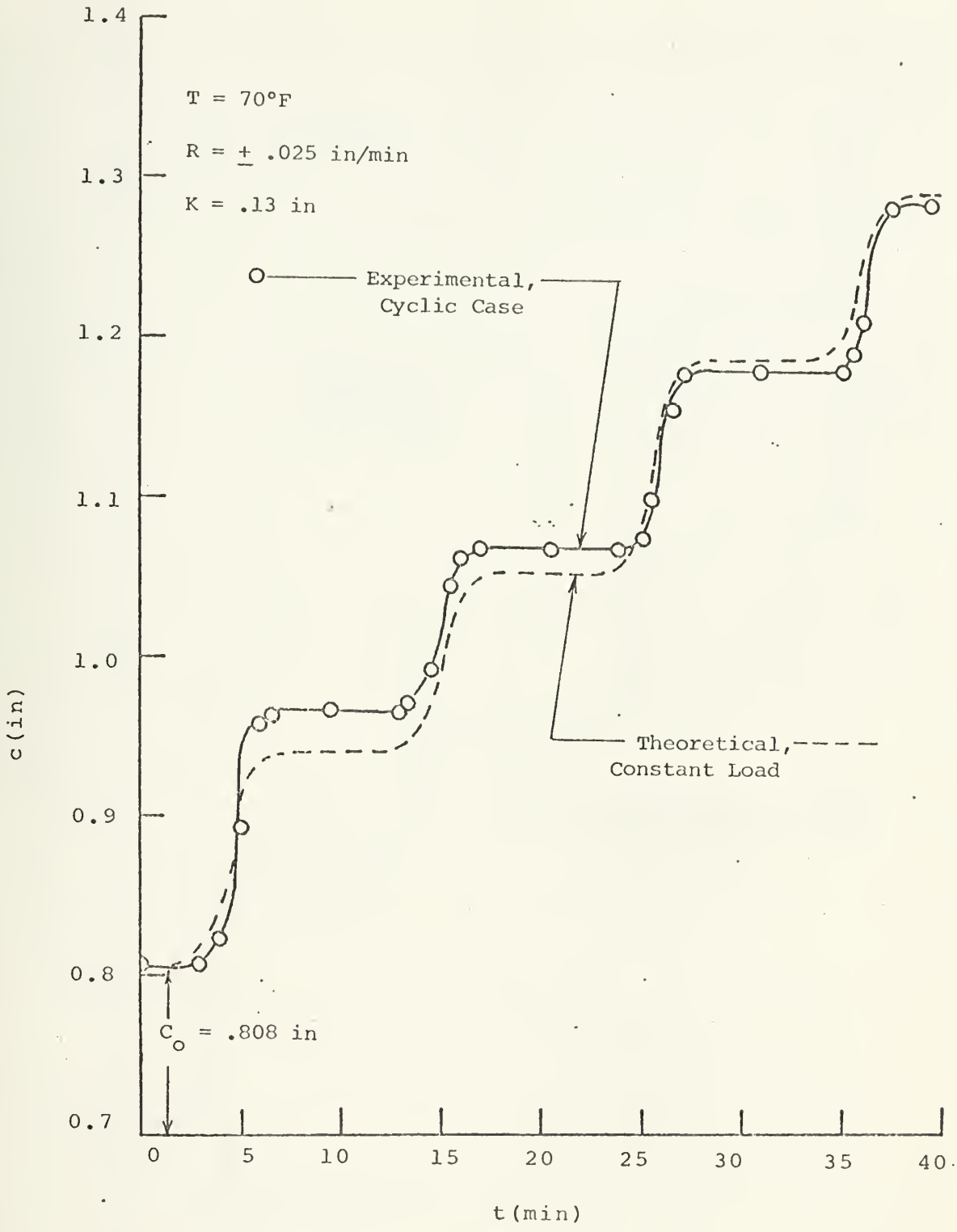

Figure 15. Crack Length versus Time for the Cyclic Case.

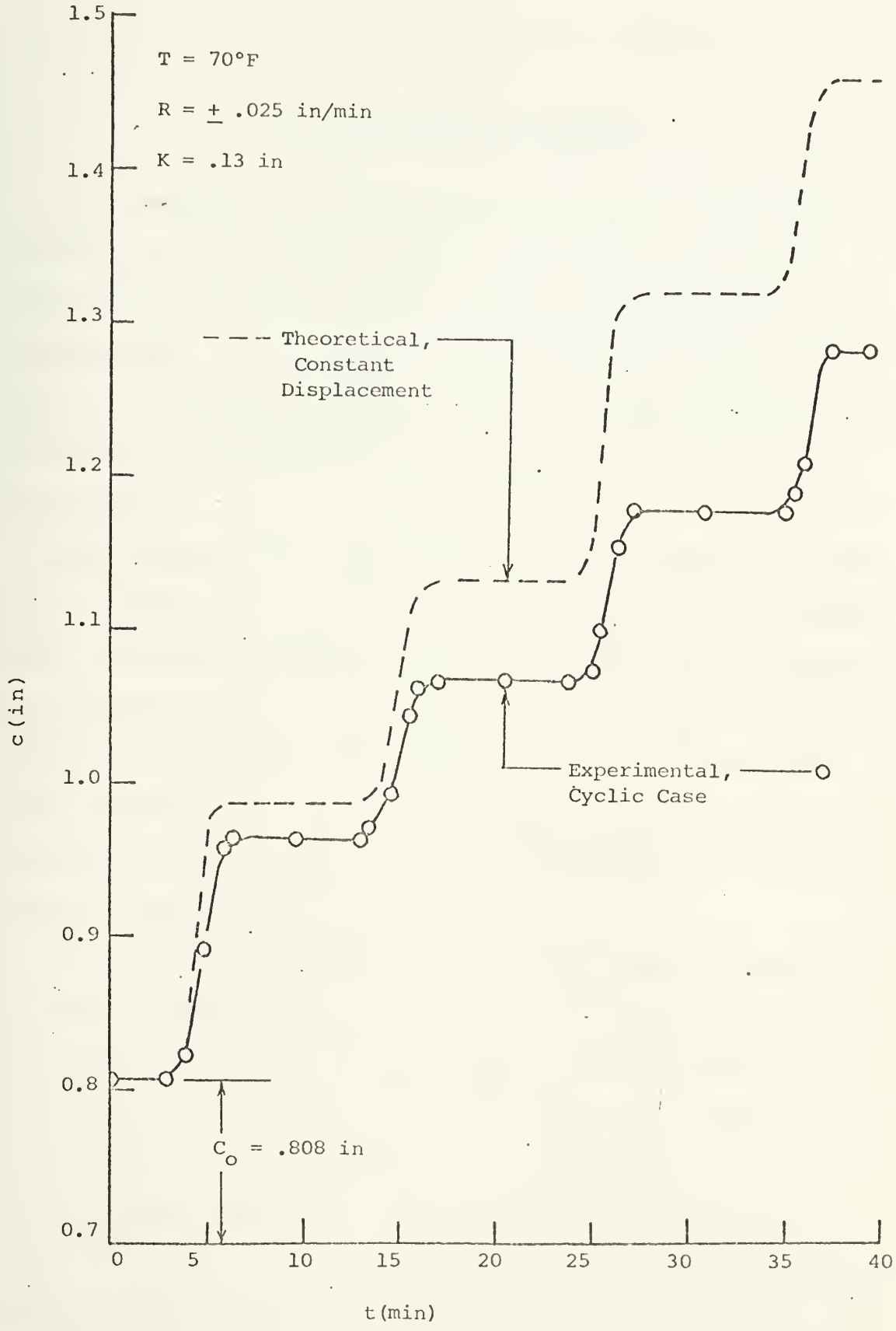

Figure 16. Crack Length versus Time for the Cyclic Case

IV. DISCUSSION OF RESULTS

The constant load, constant displacement, constant displacement rate, and cyclic tests were diverse in nature, each having several positive aspects and some having minor deficiencies. Each of these four tests probed different aspects of material behavior, and collectively they provided a thorough and comprehensive examination of the fracture postulate.

The constant load case had two positive features. The test occurred over a relatively long period of time, simplifying laboratory techniques and stabilizing test conditions, and the theoretical stress intensity factors were independent of external relaxation data. Detracting from this test, however, was the mechanical apparatus used to apply a constant load. Unless carefully manipulated, it would induce a moment at the crack tip.

The constant displacement case had several attractive features. Stress intensity factors were calculated using relaxation data obtained from constant displacement tests. Since the test material was an elastomer, the reduction in crack velocity due to relaxation occurred over a substantially longer time than a similar test using solid propellant. Hertzler [Ref. 2] found this test virtually impossible to use for propellants because rapid relaxation caused the crack velocities to go to zero before data

could be taken. Finally, the Instron was capable of a consistent application of the constant displacement case.

The constant displacement rate case utilized the Instron in its most fundamental mode of operation. Since few tests were required for fracture characterization, these tests were repeated. Excellent consistency was obtained between like tests. A primary disadvantage was that the stress intensity factor calculation required relaxation data. The only relaxation data available were those obtained from a constant strain case.

The comments pertaining to the constant displacement rate case were relevant to the cyclic case. The cyclic case was a more thorough test, however, as disparities between experimental and theoretical results were accumulated over each cycle, and a discrepancy not apparent in one cycle (equivalent to one constant displacement rate test) was apparent after several cycles.

The summary of the master fracture characterization curves given in Figure 10 graphically compares the constant displacement, constant load, and constant displacement rate cases. This shows a correlation of results among the three tests within an error band of $\pm$7% measured on the vertical. Figure 11, Figure 12, and Figure 13 compares the three constant displacement rate cases with the constant load case and the constant displacement case using the incremental technique. These results were consistent with Figure 10, as moderate correlation was

obtained in all test cases. Figure 15 and Figure 16 compare the cyclic case with the constant load case and the constant displacement case, respectively, using the incremental technique. The cyclic test had good correlation with the constant load test through four cycles. It would be difficult to maintain this agreement through a large number of cycles, however, as the incremental process resulted in the error in one cycle being added to succeeding cycles. This manifestation of the cyclic test is illustrated in Figure 16 where the constant displacement and constant displacement rate cases became further separated with increasing cycles, because only a moderate agreement existed between the two test cases in any one cycle.

The analytical theory used in obtaining viscoelastic stress intensity factors was based upon linear theory in that the change in the sample dimensions, when it was loaded, was assumed to be small. In actual test cases, however, specimens experienced from 20% to 40% strain, causing considerable variation in sample width and thickness. This represented a significant departure from the linear case.

A second departure from the analytical theory occurred when the crack developed a finite crack tip radius. The classical theory for the stress intensity factor was developed for an infinitely sharp crack. When the unfilled viscoelastic test specimens were loaded, however, the crack

tip was approximately elliptic. Figure 17 shows two specimens at different strains under typical loading situation. These photographs indicate not only a finite crack tip radius but also a change in radius with a corresponding change in material strain. Since the concept of a stress intensity factor as a function of crack tip radius has not been developed, one can only speculate on its effect.

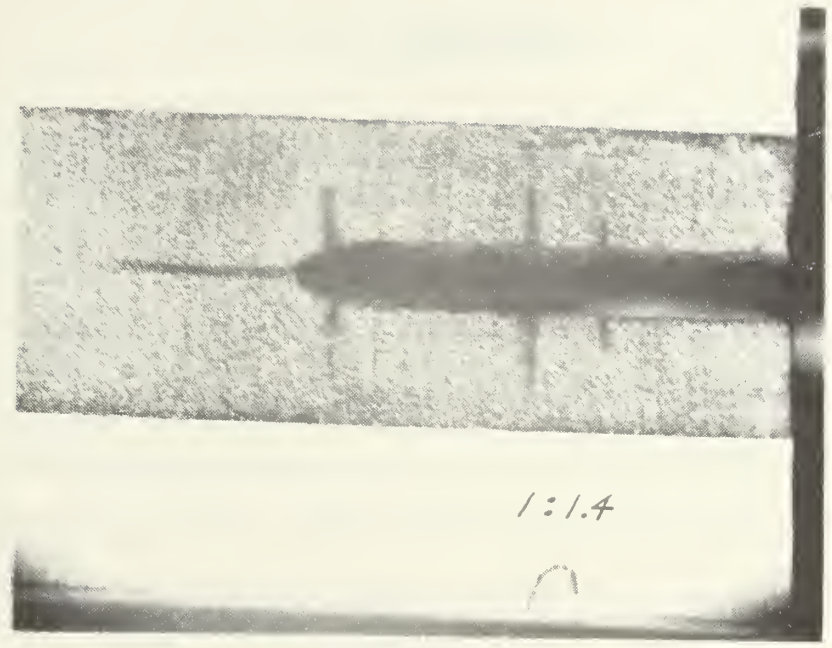

a. $\varepsilon = .225$, $\rho \cong .0425$ in, $T = 70^{\circ}F$

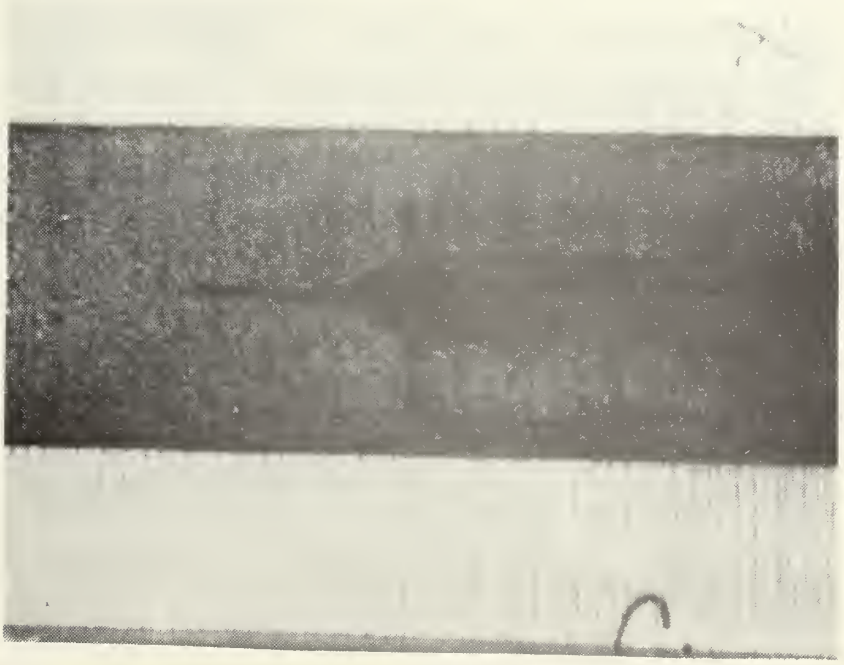

b, $\varepsilon = .275$, $\rho \cong .053$, $T = 70^{\circ}F$

Figure 17. Typical Crack Geometries.

V. CONCLUSION

The moderate correlation among the constant load, constant displacement, constant displacement rate, and cyclic test cases tended to support the fracture postulate and gave credence to Hertzler's argument concerning dewetting. Test results, however, lacked absolute agreement as there was a 15% spread among the fracture characterizations for the four test cases. This disparity was primarily attributed to the nonlinearities inherent in the experimental tests. The effect of a finite crack tip radius on stress intensity factor was not known, but its influence did not appear to be large since only a small range of crack tip radii were present in the experimental tests.

The fracture postulate would appear to be even more applicable to propellant, assuming the dewetting phenomenon could be incorporated into the fracture theory, because the relatively stiff nature of propellant and the constraints imposed by the rocket motor structure would limit material strains within the linear assumptions used in the fracture postulate.

REFERENCES

1. Naval Postgraduate School - 57Ll73031A, Viscoelastic Analysis Method for Rocket Motors Containing Cracks, by Gerald H. Lindsey, March 1973.

2. Hertzler, Charles Miller, Viscoelastic Fracture Characterization of a Solid Propellant, A. E. Thesis, Naval Postgraduate School, Monterey, California, June 1972.

3. Chemical Propulsion Information Agency Publication 21, ICRPG Solid Propellant Mechanical Behavior Manual, The John Hopkins University Applied Physics Laboratory, Silver Spring, Maryland, September 1963.

INITIAL DISTRIBUTION LIST

		No. Copies
1.	Defense Documentation Center Cameron Station Alexandria, Virginia 22314	2
2.	Library, Code 0212 Naval Postgraduate School Monterey, California 93940	2
3.	Associate Professor G. H. Lindsey Department of Aeronautics Naval Postgraduate School Monterey, California 93940	3
4.	Lieutenant Robert Edwin Kapernick, USN 3239 Villa Circle Marina, California	1
5.	Chairman Department of Aeronautics Naval Postgraduate School Monterey, California 93940	1

SECURITY CLASSIFICATION OF THIS PAGE (When Data Entered)

REPORT DOCUMENTATION PAGE		READ INSTRUCTIONS BEFORE COMPLETING FORM
1. REPORT NUMBER	2. GOVT ACCESSION NO.	3. RECIPIENT'S CATALOG NUMBER
4. TITLE (and Subtitle) Evaluation of the Fracture Postulate for Viscoelastic Materials		5. TYPE OF REPORT & PERIOD COVERED Master's Thesis December 1973
		6. PERFORMING ORG. REPORT NUMBER
7. AUTHOR(s) Robert Edwin Kapernick		8. CONTRACT OR GRANT NUMBER(s)
9. PERFORMING ORGANIZATION NAME AND ADDRESS Naval Postgraduate School Monterey, California 93940		10. PROGRAM ELEMENT, PROJECT, TASK AREA & WORK UNIT NUMBERS
11. CONTROLLING OFFICE NAME AND ADDRESS Naval Postgraduate School Monterey, California 93940		12. REPORT DATE December 1973 13. NUMBER OF PAGES 41
14. MONITORING AGENCY NAME & ADDRESS(If different from Controlling Office) Naval Postgraduate School Monterey, California 93940		15. SECURITY CLASS. (of this report) Unclassified 15a. DECLASSIFICATION/DOWNGRADING SCHEDULE

16. DISTRIBUTION STATEMENT (of this Report)

Approved for public release; distribution unlimited.

17. DISTRIBUTION STATEMENT (of the abstract entered in Block 20, if different from Report)

18. SUPPLEMENTARY NOTES

19. KEY WORDS (Continue on reverse side if necessary and identify by block number)

Fracture
Viscoelastic Fracture
Elastomer Fracture

20. ABSTRACT (Continue on reverse side if necessary and identify by block number)

Experimental studies were conducted on unfilled viscoelastic materials to evaluate the fracture postulate which states that crack velocity is a unique function of stress intensity factor. To do this, fracture characterization tests were conducted for constant load, constant displacement, and constant displacement rate histories. A cyclic study, a more sophisticated application of the constant displacement rate case, was

DD FORM 1 JAN 73 1473 EDITION OF 1 NOV 65 IS OBSOLETE
S/N 0102-014-6601 |
(Page 1)

SECURITY CLASSIFICATION OF THIS PAGE (When Data Entered)

also conducted as a further evaluation of the fracture postulate.

The analytical theory used in obtaining viscoelastic stress intensity factors was based upon linear theory and sharp crack geometries. Moderate correlation was obtained among all test cases, notwithstanding the presence of significant specimen strains and finite crack tip radii.